Soft Matter

Cite this: *Soft Matter*, 2011, **7**, 3844

www.rsc.org/softmatter

PAPER

The effect of self-assembled nanofibrils on the morphology and microstructure of poly(L-lactic acid)

Wei-Chi Lai*[ab]

Received 17th October 2010, Accepted 31st January 2011
DOI: 10.1039/c0sm01170c

The morphologies and microstructures of neat 1,3:2,4-dibenzylidene-D-sorbitol (DBS) and DBS/poly(L-lactic acid) (PLLA) samples have been investigated by polarizing optical microscopy (POM) and scanning electron microscopy (SEM). The morphology of neat DBS samples prepared from solution had unspecific structures, and no fibrils formed. In comparison, DBS molecules self-assembled into fibrils with diameters ranging from 100 nm to 1 μm when samples were prepared from the melt. The DBS fibrils were also found in DBS/PLLA systems, but the average diameter was only around 20 nm. The DBS architectures could be well tuned by varying the DBS contents and PLLA crystallization temperatures. Micron-sized fibrillar rings or disks due to the aggregation of DBS nanofibrils were found using SEM in samples with DBS contents more than 3 wt% and crystallized above 120 °C. Meanwhile, "concentric-circled" PLLA spherulites were observed by POM. The DBS nanofibrils largely formed at the circles, but some nanofibrils formed beyond the circles and were dispersed in the PLLA spherulites. These dispersed nanofibrils affected the orientation of PLLA lamellae and caused a change in birefringence, yet the growth rate of PLLA was not significantly influenced by the formation of DBS nanofibrils. In addition, porous PLLA structures could be obtained by solvent extraction of the DBS nanofibrils.

Introduction

1,3:2,4-Dibenzylidene sorbitol (DBS) is an amphiphilic molecule, which is derived from the sugar alcohol D-glucitol. Fig. 1 displays the chemical structure of DBS. DBS could self-assemble into nanofibrils through the hydrogen bonding in a wide variety of organic solvents and liquid polymers.[1–6] Electron microscopy and atomic force microscopy show that the diameter of these DBS nanofibrils generally ranges from 10 nm to 0.8 μm. On the other hand, the microstructures of neat DBS prepared from the melt have been also discussed.[6] The diameter of neat DBS fibrils, ranging from 100 nm to 1 μm, is much larger than that of DBS nanofibrils found in organic solvents or liquid polymers. In some cases, DBS molecules dissolved in organic media can cause physical gelation. The resulting materials are a type of "organogels". The DBS organogels could provide some applications such as gel antiperspirants, gel electrolytes, cosmetics and so on.[7–9] Recently, Wilder *et al.*[10,11] reported the preparation of dental composites with improved mechanical strength by utilizing the organogel formed in dental monomers including an ethoxylated bisphenol A dimethacrylate (EBPADMA).

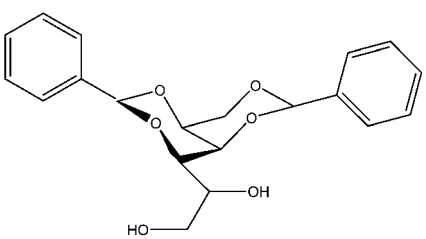

Fig. 1 Chemical structure of 1,3:2,4-dibenzylidene-D-sorbitol (DBS).

In our earlier studies,[12] DBS organogels were used as self-assembled scaffolds for preparing polystyrene (PS) nanocomposites and porous materials. DBS molecules were dissolved in styrene/initiator mixtures at high temperature. After cooling to room temperature, DBS organogels were obtained as a result of the DBS nanofibrillar networks formed. The PS materials with DBS nanofibrils were then synthesized using thermal-initiated polymerization. DBS nanofibrils could act as reinforcing materials for improved mechanical properties. In addition, the porous PS materials were prepared by the solvent extraction of DBS nanofibrils.

The sample preparation here is much easier than that in our previous studies: DBS and a crystalline polymer, poly(L-lactic acid) (PLLA), were directly blended by solution casting. We found that DBS nanofibrils can form after heat treatments. In

[a]*Department of Chemical and Materials Engineering, Tamkang University, 151 Ying-chuan Road, Tamsui, Taipei, 25137, Taiwan. E-mail: wclai@mail.tku.edu.tw; Fax: +886-2-2620-9887; Tel: +886-2-2621-5656 ext. 3516*
[b]*Energy and Opto-Electronic Materials Research Center, Tamkang University, 151 Ying-chuan Road, Tamsui, Taipei, 25137, Taiwan*

addition, we also discussed how the formation of DBS nanofibrils affected the morphologies and microstructures of the crystalline polymer. Recently, many researchers have used DBS as a nucleating agent to change the crystallization rate and optical properties of crystalline polymers, such as polyethylene and polypropylene.[13–15] Though some reported the observation of the DBS fibrils in these polymers, there is no detailed discussion on the microstructures or the formation process of the DBS fibrils. Here, we investigated the microstructures and morphologies of DBS/PLLA systems by SEM and POM. Our results show that the aggregated structures of DBS nanofibrils could be controlled by the change in DBS amounts and PLLA crystallization temperatures. Furthermore, the structure and morphology of neat DBS samples prepared from solution were also discussed, on which little information is available.

The temperature range of the formation of DBS fibrils was very close to that of crystallization temperature of PLLA spherulites. The temperature range for DBS fibrils formation depends on the DBS concentration and cooling/heating rate. Usually, the range is between 100 and 200 °C. Therefore, in this study, we examined the interaction between DBS fibrils and PLLA crystals as well. Moreover, we attempted to prepare porous PLLA materials by the removal of DBS nanofibrils. PLLA has attracted much attention due to their potential applications as biomedical and green materials,[16–18] and such porous PLLA materials could be used as scaffolds for the cell transplantation and tissue regeneration.[19] There are a lot of ways to prepare porous PLLA films, such as solution-casting-leaching, thermal precipitation, solvent evaporation, immersion precipitation, and so on.[20–24] The method proposed here might provide useful information on the fabrication of porous PLLA of different morphologies.

Experimental

Materials

DBS (1,3:2,4-dibenzylidene-D-sorbitol) was obtained from Milliken Chemicals. PLLA (poly(L-lactic acid)) was purchased from NatureWorks. The molecular weight and polydispersity of PLLA determined by GPC are 58 000 g mol^{-1} and 1.73. Ethanol was of reagent grade and was obtained from Fluka.

Sample preparation

The neat DBS samples were prepared by dissolving 0.08% (w/v) DBS in chloroform at room temperature under constant agitation. After the DBS was completely dissolved, the solution was subsequently poured onto a glass plate. A film was obtained after evaporating chloroform solvent very slowly under ambient conditions at room temperature. The film was then further dried in vacuum at 80 °C for 24 hours. Also, TGA was used to check the residual solvent in the final films. The results showed no measurable residual solvent in the films.

Preparation of DBS/PLLA samples was also carried out by solution casting. DBS and PLLA were dissolved in chloroform yielding a 2% (w/v) solution. The DBS contents in DBS/PLLA samples were 0, 1, 2, 3 and 4 wt%. As the DBS amount was increased to 5 wt%, DBS could not dissolve completely, and only opaque solution was observed. Therefore, the DBS contents ranging from 0 to 4 wt% were chosen for the following investigations.

The molecular interactions between DBS and PLLA were determined using Fourier transform infrared (FTIR) spectroscopy (NICOLET iS10). The samples were dissolved in chloroform yielding a 2% (w/v) solution, cast onto KBr plates, and then dried in vacuum.

Porous PLLA samples were prepared by solvent extraction of the DBS nanofibrils. The DBS was washed by the ethanol for a week. The removal was confirmed by a Bruker AC300 FT-nuclear magnetic resonance spectrometer (NMR). NMR spectra were measured in chloroform-d with tetramethylsilane (TMS) as an internal standard.

Polarized optical microscopy

The morphologies of neat DBS and DBS/PLLA samples were observed using a Precisa XT-200A polarized optical microscope (POM) with a compensator. Neat DBS or DBS/PLLA solution was dropped onto a glass pate, and the films would be obtained after the evaporation of the solvent. The samples were then put in vacuum at 80 °C for 24 hours. For POM experiments, the DBS/PLLA samples were fist melted on a Linkam THMS 600 hot stage equipped with a Linkam CI94 programmable temperature-controller at 200 °C for 3 minutes. The samples were quickly cooled to their crystallization temperature, where the resultant morphologies were observed until the PLLA spherulites formed completely. The spherulitic growth of DBS/PLLA samples with 3 wt% DBS crystallizing at 120 °C was observed by a POM. Micrographs were taken at interval for measuring the spherulite radii of PLLA at different time periods. The growth rate was calculated from the change of spherulite radius with time, dR/dt.

Scanning electron microscopy

The microstructures of neat DBS and DBS/PLLA samples were observed by a Leo-1530 field emission scanning electron microscope (FE-SEM). The samples prepared for the POM observation were repeatedly used in the SEM experiments. DBS/PLLA samples with 3 wt% DBS crystallized at 120 °C for different crystallization times were prepared on a hot stage equipped with a programmable temperature-controller by quenching to room temperature after 10, 20, 30 and 40 minutes of crystallization, respectively.

Results and discussion

Morphology and microstructure of neat DBS

DBS could self-assemble into nanofibrillar networks through hydrogen bonding in a range of organic solvents. Most researchers focused on the structure of DBS-induced gelation in organic solvents or low molecular weight polymers. Our previous studies have discussed the morphologies of neat DBS and DBS/poly(propylene glycol) (PPG) gels.[6] Neat DBS could self-assemble into fibrils and exhibited the spherulite-like textures during cooling from the melt, which are similar to the structures observed in DBS/PPG. However, the diameter sizes of neat DBS, ranging from 100 nm to 1 μm, are much larger than those of DBS/PPG gels. In this study, we focus on the morphology and

microstructure of neat DBS samples prepared from solution, on which no references are available to our knowledge. The samples were prepared by dissolving small amounts of DBS in chloroform and solution casting (details in Experimental section). Fig. 2(a) and (c) display the POM and SEM micrographs of neat DBS samples prepared by solution casting at room temperature. These structures were quite different from those of neat DBS prepared from the melt.[6] No distinct, birefringent spherulite-like morphology was observed by POM (Fig. 2(a)). POM photograph shows that the aggregations of DBS scattered over the surface of the substrate. The structure of the aggregated (or concentrated) DBS molecules was more irregular than that of neat DBS prepared from the melt,[6] and no fibrils were observed by SEM (Fig. 2(c)). Also, there were no fibrillar networks. These samples were then heated up to 200 °C at a rate of 10 °C min^{-1} and cooled to room temperature. Fig. 2(b) and (d) demonstrate the POM and SEM micrographs of the solution-cast samples after the heat treatment. The fibrils formed around 185 °C, and the overall growth was similar to that of the typical spherulites from the POM observation. However, the change in birefringence was not obvious. The DBS molecules could self-assemble into fibrils and the diameters of the aggregated fibrils ranged from 100 nm to 1 μm by SEM, which was very similar to those of neat DBS prepared from the melt.[6] Thus, the condition for DBS fibril formation seems to be that the number of aggregated DBS molecules has to be large enough. At high temperature, the DBS molecules start to move and easily aggregate together due to the existence of hydrogen bonding between DBS because of the hydroxyl groups, and therefore the DBS fibrils would form (see Fig. 2(b) and (d)). On the other hand, if DBS molecules are less aggregated, no fibrils form and only irregular shapes can be observed (see Fig. 2(a) and (c)).

Morphology and microstructure of DBS/PLLA

The DBS/PLLA samples prepared using the same procedure by solution casting. The DBS contents in the solutions of DBS/PLLA samples were similar to those in the solutions of neat DBS.

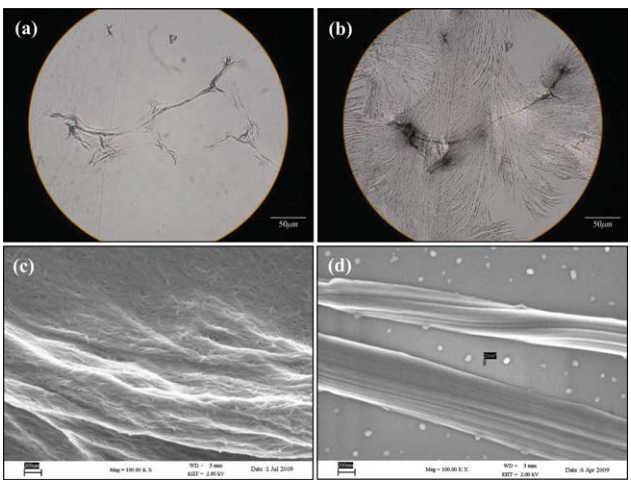

Fig. 2 POM micrographs of neat DBS samples prepared by solution casting (a) at room temperature and (b) after the heat treatment. The respective SEM micrographs are shown in (c) and (d).

Nevertheless, neither DBS fibrils nor irregular structures of aggregated DBS were found by POM and SEM in the DBS/PLLA samples after casting. Only PLLA spherulites appeared. Moreover, when the samples were heated up to 185 °C, the PLLA spherulites melted (the melting point of PLLA determined by differential scanning calorimetry is around 160 °C), but there was still no DBS fibril formation. Therefore, it is believed that there could be some interactions between DBS and PLLA limiting the formation of DBS fibrils in DBS/PLLA systems.

Since the formation of DBS fibrils was not observed during the same heat treatment used for neat DBS samples, we tried other treatment conditions. In addition, at lower temperatures, the PLLA spherulites would appear, and it should be interesting to investigate the competition between the growth of PLLA spherulites and that of DBS fibrils if the DBS fibrils could form in such situations. Hence, a series of DBS/PLLA samples with DBS contents of 0–4 wt% were prepared, and the samples were heated to 200 °C and then quickly cooled to different temperatures, 90–140 °C, for PLLA to crystallize. Intriguingly, as the samples contained at least 3 wt% DBS and the crystallization temperature was above 120 °C, new structures were found using POM (Fig. 3(a)): concentric circles in PLLA spherulites. It was unlike the typical spherulites of PLLA or the ringed-banded spherulites,[25] which had periodic extinction rings. In comparison, the circles appeared only once. We call the new PLLA structures "concentric-circled spherulites". The spherulitic morphologies and microstructures of samples with 3 wt% DBS at 120 °C by POM and SEM are shown in Fig. 3(a) and (b), where the identical sample was used. Labels 1, 2, 3 and 4 in both photographs mark the spherulites to be examined. It was found that most of the fibrils aggregated around the concentric circles. Moreover, the size of fibrils in DBS/PLLA system was "nano-scaled" (so we would call them "nanofibrils"). The size was very different from that in the neat DBS system. However, the size of DBS nanofibrils was quite close to those of DBS in organic solvents or liquid polymers,[1,2] and these systems all exhibited the 3-D nanofibrillar networks.

Samples crystallized at 120 °C with 0–2 wt% DBS exhibited typical PLLA spherulites, and samples with 3 and 4 wt% DBS had concentric-circled spherulites as observed by POM. No ring-banded structures were found (POM photographs are not shown). Fig. 4 displays a series of SEM photographs of DBS/PLLA samples with different DBS contents crystallized at 120 °C. The positions of aggregated DBS nanofibrils are related

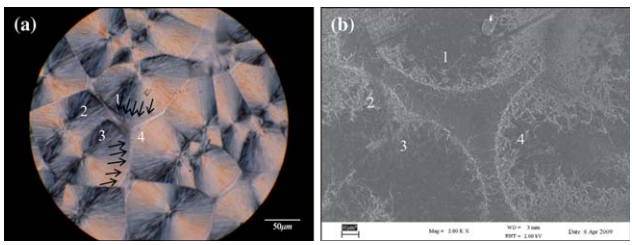

Fig. 3 (a) POM and (b) SEM micrographs of the spherulitic morphology and microstructure of PLLA samples with 3 wt% DBS crystallized at 120 °C, where labels 1, 2, 3 and 4 in both photographs mark the spherulites to be examined. Some of the concentric circles are indicated by arrows.

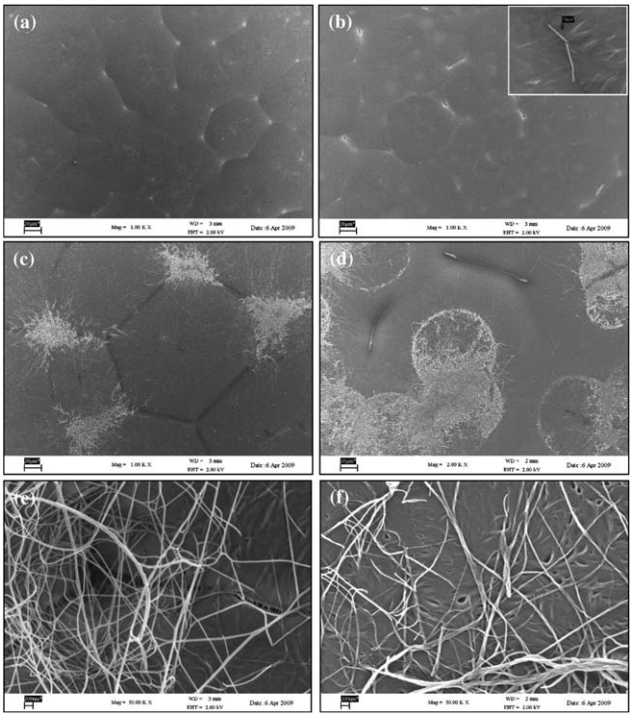

Fig. 4 A series of SEM photographs of DBS/PLLA samples crystallized at 120 °C with (a) 0, (b) 1, (c) 2, and (d) 4 wt% DBS. Areas where the nanofibrils aggregated in (c) and (d) are shown in (e) and (f) at higher magnification (50 000×). The inset in (b) is at 100 000×.

to the contents of DBS. Few DBS nanofibrils were observed in the sample with 1 wt% DBS. However, a large amount of DBS nanofibrils formed as DBS content reached 2 wt% (see Fig. 4(c)). The fibrils segregated between spherulites, but POM showed no obvious differences. Moreover, the PLLA spherulites almost completely filled the space at the final crystallization stage. It seemed that the aggregated DBS nanofibrils formed after the PLLA crystallization, and thus hardly influenced the growth of PLLA spherulites.

When the concentration of DBS reached 3 and 4 wt%, the fibrils aggregated to form circles inside spherulitic regions (Fig. 3(b) and 4(d)). The concentric-circled structures were also observed by POM. The DBS aggregated structures were different from those in samples with 2 wt% DBS. The DBS nanofibrils in samples containing 3 and 4 wt% DBS aggregated into μm sized "fibrillar rings" or "fibrillar disks." The high-magnification SEM micrographs of samples containing 2 and 4 wt% DBS are shown in Fig. 4(e) and (f). Independent of the location of the DBS self-assembled inside or outside spherulitic regions, the diameter sizes of these nanofibrils ranged from 10 nm to 200 nm, and the average diameter size was near 20 nm. Furthermore, the average diameter of the DBS fibrillar rings and disks in samples containing 3 wt% DBS was around 100 μm (Fig. 3(b)). In addition, the average diameter of fibrillar rings and disks in samples with 4 wt% DBS was about 50 μm (Fig. 4(d)).

Fig. 5 displays a schematic representation of the DBS/PLLA samples with different DBS contents crystallized at 120 °C. As the PLLA crystallizes, DBS molecules are excluded outside the crystals; hence the concentration of DBS in the amorphous

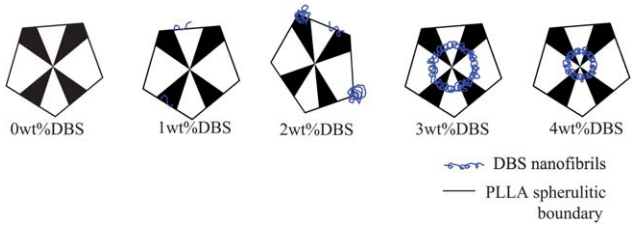

Fig. 5 A schematic representation of the DBS/PLLA samples with different DBS contents crystallized at 120 °C.

region increases. It is supposed that the local DBS concentration must be high enough to form the nanofibrils. Thus, at 1 wt% DBS, few nanofibrils form. As the DBS content reaches 2 wt%, the local concentration of DBS is still not sufficient at the early stages of PLLA crystallization. However, when the PLLA crystallization is complete, the concentration of DBS molecules ejected outside the PLLA crystals is relatively high. As a result, DBS molecules self-assemble to form the nanofibrils between spherulites. On the other hand, as the DBS contents are 3 and 4 wt%, the formation of nanofibrils is much easier due to the higher DBS contents. Therefore, DBS nanofibrils form earlier during the PLLA crystallization process and aggregate inside the spherulites. Moreover, the formation of DBS nanofibrils in samples containing 4 wt% DBS is much earlier than that in samples containing 3wt% DBS due to the higher DBS contents, which is evident in SEM observations. The average diameter of the fibrillar rings or disks (the primary location where DBS nanofibrils aggregate) in samples with 4 wt% DBS was much smaller than that in samples with 3 wt% DBS (Fig. 3(b) and 4(d)).

The structures of aggregated fibrils could be finely controlled not only by the different amounts of DBS but also by the PLLA crystallization temperatures. For example, as the samples containing 3 wt% DBS were crystallized at temperatures higher than 120 °C, the concentric-circled structures could be observed (see Fig. 6(b)). That is, the DBS molecules aggregated inside the spherulites. When the crystallization temperature was lower than 120 °C, few concentric-circled spherulites were found, and most of the DBS nanofibrils aggregated outside the spherulites (see Fig. 6(a)). As the crystallization temperature was increased, PLLA crystallization rate decreased, and DBS molecules were excluded by PLLA crystals more easily, leading to a significant increase in the DBS concentration at the crystal front. Thus, DBS nanofibrils formed earlier in the PLLA crystallization process, which resulted in the concentric-circled structures. In

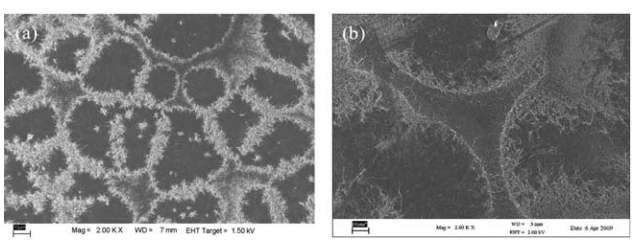

Fig. 6 SEM photographs of DBS/PLLA samples with 3 wt% DBS crystallized at (a) 100 °C and (b) 120 °C.

contrast, DBS concentration was high enough only near the end of PLLA crystallization at lower crystallization temperatures, and DBS nanofibrils were mostly found at the spherulitic boundaries.

In addition, the concentrations of aggregated DBS molecules have to be high enough for the fibrils to form in both the neat DBS and DBS/PLLA systems. However, the sizes of fibrils in the two systems were quite different. The fibril diameter of neat DBS was much larger than that in DBS/PLLA systems. It is possible that some interactions (such as hydrogen bonding) between PLLA and DBS interfere the aggregation of DBS molecules. As a result, DBS "nanofibrils" were found in DBS/PLLA systems.

FTIR spectroscopy was used to determine if there are intermolecular interactions between DBS and PLLA. Fig. 7 shows FTIR spectra of DBS, PLLA and DBS/PLLA samples with 4 wt% DBS. The C=O stretching band in PLLA sample at 1755 cm^{-1} was much broader as DBS was added. It is known that the hydrogen bonding would affect the molecular vibrations of nearby groups,[26] which may cause such a broadening. The result indicates that there was hydrogen bonding between DBS and PLLA.

Formation process of DBS nanofibrils in DBS/PLLA

We attempted to observe the formation process of DBS nanofibrils in DBS/PLLA systems during PLLA crystallization, in particular, when the DBS fibrils formed, and discussed the cause of the concentric-circled structures in this system. The DBS/PLLA samples of 3 wt% DBS were prepared by quenching the samples crystallized at 120 °C for different periods of time (0, 10, 20, 30 and 40 minutes). Fig. 8 and 9 show the POM and SEM photographs of these samples. As can be seen in Fig. 8, typical spherulites of PLLA were found in samples crystallized for less than 30 minutes, whereas concentric-circled PLLA spherulites appeared in samples crystallized for 40 minutes. SEM observations (Fig. 9) show that a considerable amount of the DBS nanofibrils formed after the appearance of concentric-circled structures. For clarity, regions were labeled A, B and C in Fig. 8 and 9, where A means the region inside a PLLA spherulite or inside the circle within a concentric-circled spherulite, B represents the region outside the circle within a concentric-circled spherulite, and C is the amorphous PLLA region. As PLLA crystallized for 20 minutes, few DBS fibrils were found in regions A and C. The morphology in region A was typical of PLLA

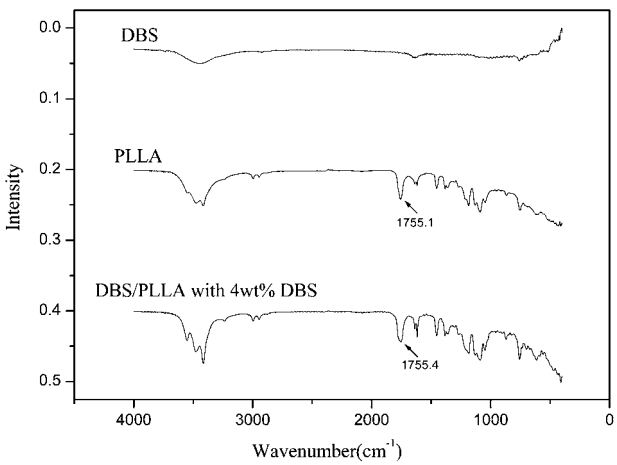

Fig. 7 FTIR spectra of DBS, PLLA and DBS/PLLA samples with 4 wt% DBS.

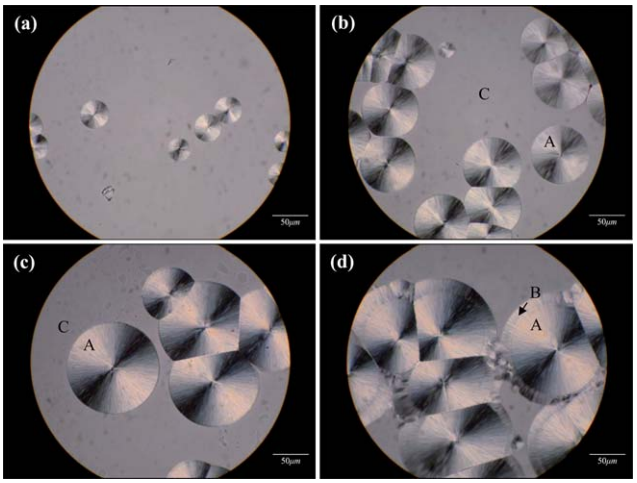

Fig. 8 POM photographs of DBS/PLLA samples with 3 wt% DBS crystallized at 120 °C for (a) 10, (b) 20, (c) 30, and (d) 40 minutes, where label A means the region inside a PLLA spherulite or inside the circle within a concentric-circled spherulite, B represents the region outside the circle within a concentric-circled spherulite, and C is the amorphous PLLA region.

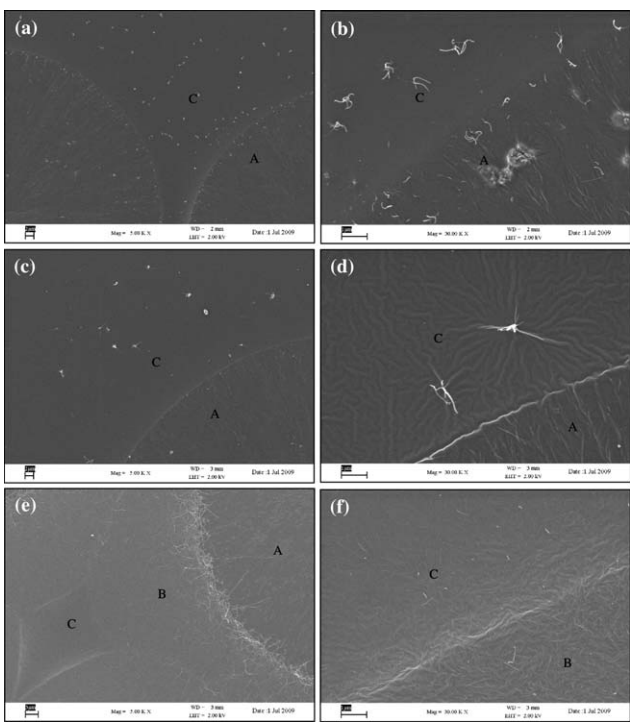

Fig. 9 SEM photographs of DBS/PLLA samples with 3 wt% DBS crystallized at 120 °C for (a) 20, (c) 30, and (e) 40 minutes (5000×). (b), (d), and (f) are at higher magnification (30 000×), where the meaning of labels A, B and C is the same as that in Fig. 8.

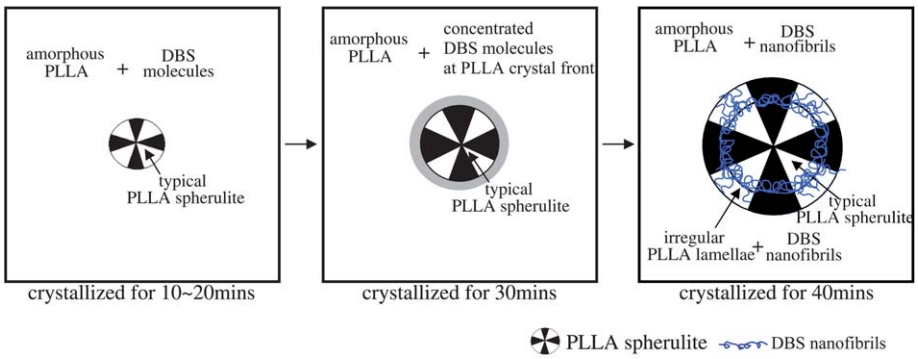

Fig. 10 A schematic representation of the formation of DBS nanofibrils during the crystallization of PLLA.

spherulites, and region C exhibited a smooth and flat surface (see Fig. 9(a) and (b)). However, after PLLA crystallized for 30 minutes, region C became irregular and rough, which may be caused by the increased number of aggregated DBS molecules. Meanwhile, region A still exhibited the typical PLLA spherulites (see Fig. 9(c) and (d)). When PLLA crystallized for 40 minutes, region B appeared. The DBS nanofibrils largely formed at the circle (between regions A and B), and some nanofibrils were still found in regions B and C. Note that region B was much irregular than region A (see Fig. 9(e) and (f)).

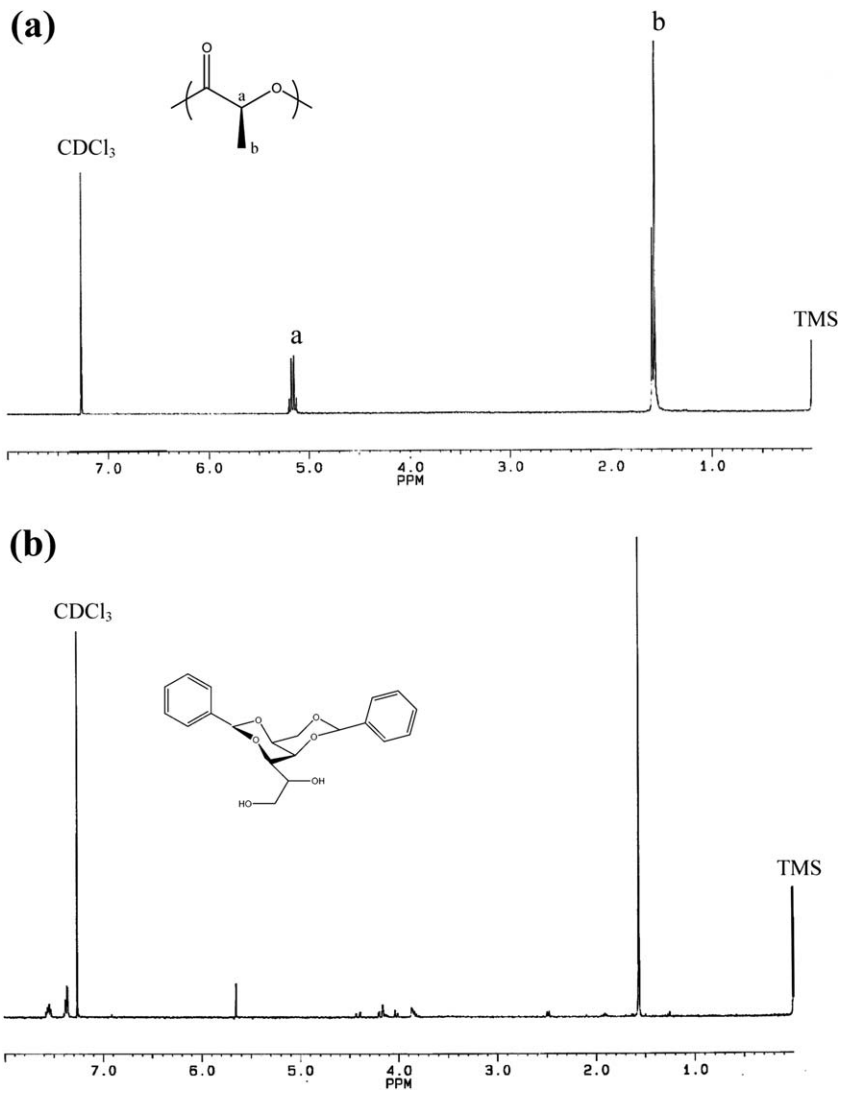

Fig. 11 NMR spectra of (a) the sample after washing and (b) a neat DBS sample.

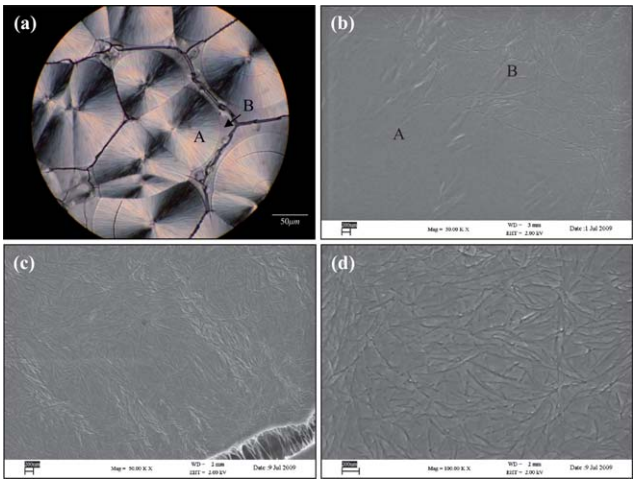

Fig. 12 (a) POM and (b) SEM photographs of the DBS/PLLA samples crystallized at 120 °C with 3 wt% DBS after extraction by ethanol, where label A means the region inside a PLLA spherulite or inside the circle within a concentric-circled spherulite, B represents the region outside the circle within a concentric-circled spherulite. (c and d) show an area near the spherulitic boundary of the sample at magnification 50 000× and 100 000×, respectively.

The above observation is summarized in Fig. 10, which displays a schematic representation of the formation of DBS nanofibrils during the crystallization of PLLA. In the first 20 minutes of PLLA crystallization, the amount of aggregated DBS molecules are small, and the DBS molecules can be easily excluded by the PLLA crystals. Thus, the PLLA crystals are typical spherulites. As the crystallization time increases, more DBS molecules aggregate at the PLLA growth front. As a result, the irregular and rough morphology of aggregated DBS can be seen. However, the increased concentration of DBS is still not high enough for a large amount of DBS nanofibrils to form. During the crystallization time between 30 and 40 minutes, the aggregated DBS molecules are sufficient to form the nanofibrils at the PLLA growth front. Hence, the fibrillar rings or disks appear. These results are coincident with what we found in neat DBS. In addition, the formation of DBS nanofibrils seems to influence the PLLA spherulites. The structures inside and outside the circle within a concentric-circled spherulite were quite different. The detailed observation will be discussed in the next section.

Porous PLLA materials prepared by solvent extraction of DBS nanofibrils

The PLLA samples crystallized at 120 °C with 3 wt% DBS were immerged into ethanol, a good solvent for DBS, for a week to remove the DBS fibrils. Fig. 11 displays the NMR spectra of the sample after washing and a neat DBS sample. In Fig. 11(a), peaks around $\delta = 5.1$ ppm and $\delta = 1.5$ ppm can be seen, corresponding to the methylene and methyl proton resonance of the lactide.[27] That is, only neat PLLA characteristic peaks were observed after the sample was washed by ethanol. The peaks for the protons in the aromatic compounds (7.3–7.6 ppm), which are clear in the neat DBS sample (Fig. 11(b)), are absent. Therefore, the removal of DBS could be confirmed. Fig. 12, where the

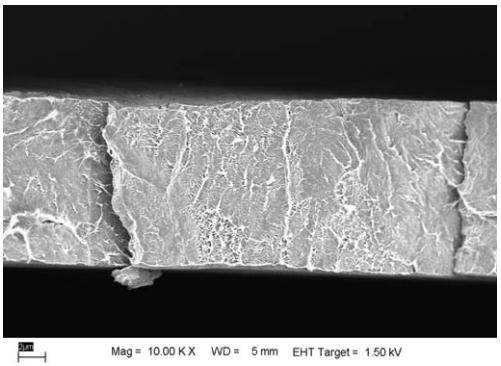

Fig. 13 A cross-sectional SEM image of a DBS/PLLA sample crystallized at 120 °C with 3 wt% DBS after DBS extraction by ethanol.

meaning of labels A and B was the same as that in Fig. 8 and 9, and Fig. 13 show the POM (top view) and SEM (top view and cross-sectional view) photographs of such a sample after DBS extraction by ethanol. As seen in Fig. 12(a), the concentric-circled PLLA spherulites could still be observed by POM, though the DBS nanofibrils were removed, as reconfirmed by SEM (Fig. 12(b)–(d)). Thus, it seems that the change in birefringence is caused by the irregular PLLA lamellae. Fig. 12(b) shows that there were no pores in region A and that the porous structure only appeared in region B. Fig. 12(c) and (d) are the SEM photographs of the same sample at different magnifications near the spherulitic boundary in region B, clearly showing the porous structure. The shape of the pores was similar to that of the DBS nanofibrils. The average diameter was around 20 nm, also very close to that of nanofibrils. Therefore, the porous structure seems to be the result of the removal of nanofibrils. The porous PLLA obtained may serve as a nanoscale scaffold, an alternate to extracellular matrix (ECM) for better cell in-growth, and be used in cell transplantation and tissue regeneration.[19,28,29] Also note that although the DBS nanofibrils could aggregate into fibrillar disks (see Fig. 3(b) and 4(d)), nanofibrils were not trapped in PLLA spherulites inside the circles. Actually, the nanofibrils seemed to be ejected out of PLLA at the circles to form the fibrillar disks. We will investigate the cause of these intriguing behaviors in our further studies.

In addition, the porous structures in region B also confirmed that some DBS nanofibrils did form beyond the circles and were dispersed in the spherulites. The dispersed nanofibrils affected the orientation of PLLA lamellae and led to a change in birefringence. As a result, the regions outside the circles in the concentric-circled PLLA spherulites were slightly different from the typical PLLA spherulites (see Fig. 8(d), for example).

Fig. 14 presents the spherulite radius of a PLLA sample with 3 wt% DBS crystallized at 120 °C as a function of time. The variation of PLLA spherulite radius with time was linear both inside and outside the circle within the same spherulite. The spherulitic growth rates ($G = dR/dt$) inside and outside the circle were 2.19 and 2.24 μm min^{-1}, respectively. The two values were very close, which means the dispersed DBS nanofibrils outside the circle did not significantly affect the PLLA growth rate. However, the growth was slightly delayed and discontinuous around the circle. Thus, it seems that the large amounts of DBS nanofibrils formed at the circle influenced the crystallization of PLLA nearby.

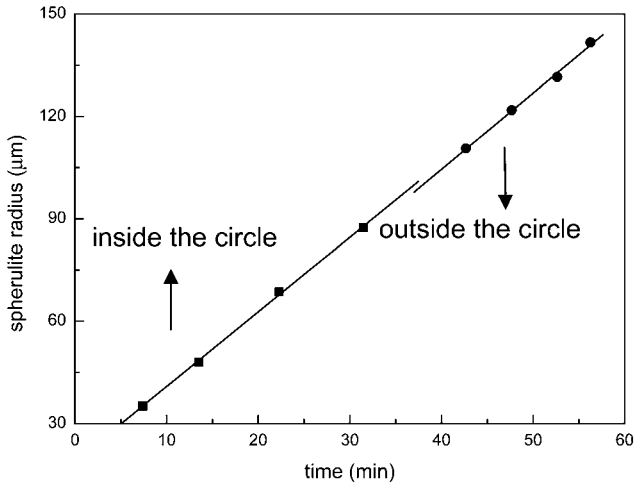

Fig. 14 The spherulite radius of a PLLA sample with 3 wt% DBS crystallized at 120 °C as a function of time.

Conclusions

The morphology and microstructure of neat DBS samples prepared from solution were different from those of the samples prepared from the melt. As the samples were prepared from solution, the DBS molecules were less aggregated, and no fibrils were observed by SEM; POM showed that there was no spherulite-like morphology. However, after the samples were heated to 200 °C and cooled to room temperature, the structures of samples became very close to those of the samples prepared from the melt. Fibrils would form, with diameters ranging from 100 nm to 1 μm. We assumed the number of aggregated DBS has to be large enough and the fibrils would form. If DBS molecules were less aggregated, only irregular shapes were observed and no fibrils formed.

The addition of DBS to PLLA resulted in different morphology and microstructure. Concentric-circled PLLA spherulites were found in DBS/PLLA systems with DBS contents larger than 3 wt% and crystallized above 120 °C. The DBS nanofibrils largely formed at the circles, but some formed beyond the circles and were dispersed in the PLLA spherulites. These dispersed nanofibrils affected the orientation of PLLA lamellae and led to a change in birefringence. Therefore, the regions outside the circles in the concentric-circled PLLA spherulites were slightly different from the typical PLLA spherulites. In addition, the formation process of DBS nanofibrils in DBS/PLLA systems was also discussed. When the PLLA crystallized, the DBS molecules were excluded by the PLLA crystals and the concentration of DBS in the amorphous region increased. As the amounts of aggregated DBS molecules were large enough, the DBS nanofibrils would form. The porous PLLA structures were obtained after the extraction of DBS nanofibrils by ethanol. The shape and average diameter of the pores were found to be similar to those of DBS nanofibrils, as observed by SEM. The PLLA growth radius of samples with time was discontinuous around the circle. The large amounts of DBS nanofibrils formed at the circle affected the crystallization of PLLA, but not significantly influenced on the PLLA growth rate.

Acknowledgements

We gratefully acknowledge financial support from the Taiwan National Science Council (NSC 99-2221-E-032-006). We also wish to thank Mr Po-Yu Chen for assisting with some of the experiments.

References

1 W. Chen, Y. Yang, C. H. Lee and A. Q. Shen, *Langmuir*, 2008, **24**, 10432.
2 E. A. Wilder, M. Braunfeld, B. H. Jinnai, C. K. Hall, D. A. Agard and R. J. Spontak, *J. Phys. Chem. B*, 2003, **107**, 11633.
3 E. A. Wilder, C. K. Hall and R. J. Spontak, *J. Colloid Interface Sci.*, 2003, **267**, 509.
4 A. Nogales, G. R. Mitchell and A. S. Vaughan, *Macromolecules*, 2003, **36**, 4898.
5 M. Kuhne and C. Friedrich, *Rheol. Acta*, 2009, **48**, 1.
6 W.-C. Lai and C.-H. Wu, *J. Appl. Polym. Sci.*, 2010, **115**, 1113.
7 N. Mohmeyer, P. Wang, H.-W. Schmidt, S. Z. Zakeeruddin and M. Gratzel, *J. Mater. Chem.*, 2004, **14**, 1905.
8 T. Schamper, M. Jablon, M. H. Randhawa, A. Senatore and J. D. Warren, *J. Soc. Cosmet. Chem.*, 1986, **37**, 225.
9 C. M. Pereira, J. M. Oliverira, R. M. Silva and F. Silva, *Anal. Chem.*, 2004, **76**, 5547.
10 E. A. Wilder and J. M. Antonucci, *Macromol. Symp.*, 2005, **227**, 255.
11 E. A. Wilder, K. S. Wilson, J. B. Quinn, D. Skrtic and J. M. Antonucci, *Chem. Mater.*, 2005, **17**, 2946.
12 W.-C. Lai and S.-C. Tseng, *Nanotechnology*, 2009, **20**, 475606.
13 M. Tenma, N. Mieda, S. Takamatsu and M. J. Yamaguchi, *J. Polym. Sci., Polym. Phys. Ed.*, 2008, **46**, 41.
14 J. Cao, K. Wang, W. Cao, Q. Zhang, R. Du and Q. Fu, *J. Appl. Polym. Sci.*, 2009, **112**, 1104.
15 K. Wang, C. Zhou, C. Tang, Q. Zhang, R. Du, Q. Fu and L. Li, *Polymer*, 2009, **50**, 696.
16 J. Hu, K. Feng, X. Liu and P. X. Ma, *Biomaterials*, 2009, **30**, 5061.
17 J. Hu, X. Liu and P. X. Ma, *Biomaterials*, 2008, **29**, 3815.
18 P. Pan, B. Zhu, W. Kai, S. Serizawa, M. Iji and Y. Inoue, *J. Appl. Polym. Sci.*, 2007, **105**, 1511.
19 A. G. A. Coombes and M. C. Meikle, *Clin. Mater.*, 1994, **17**, 35.
20 H. Tsuji and K. Suzuyoshi, *J. Appl. Polym. Sci.*, 2003, **90**, 587.
21 H. Tsuji and G. Horikawa, *Polym. Int.*, 2007, **56**, 258.
22 A. G. Mikos, A. J. Thorsen, L. A. Czerwonka, Y. Bao, R. Langer, D. N. Winslow and J. P. Vacanti, *Polymer*, 1994, **35**, 1068.
23 H. Sawalha, K. Schroen and R. Boom, *Polym. Eng. Sci.*, 2010, **50**, 513.
24 C. Yang, K. Cheng, W. Weng and C. Yang, *J. Mater. Sci.: Mater. Med.*, 2009, **20**, 667.
25 D. Shin, K. Shin, K. A. Aamer, G. N. Tew and T. P. Russell, *Macromolecules*, 2005, **38**, 104.
26 U. W. Gedde, *Polymer Physics*, Chapman & Hall, 1st edn, 1995, ch. 4, p. 71.
27 N. K. Abayasinghe, S. Glaser, K. Prasanna, U. Perera and D. W. Smith, Jr, *J. Polym. Sci., Part A: Polym. Chem.*, 2005, **43**, 5257.
28 R. G. Flemming, C. J. Murphy, G. A. Abrams, S. L. Goodman and P. F. Nealey, *Biomaterials*, 1999, **20**, 573.
29 F. Yanga, R. Murugana, S. Ramakrishnaa, X. Wang, Y.-X. Ma and S. Wang, *Biomaterials*, 2004, **25**, 1891.